Tandem Carbonylation Reactions: Hydroformylation and Hydroaminomethylation of Alkenes Catalyzed by Cationic $[(H_2C(3,5\text{-}Me_2pz)_2)Rh(CO)L]^+$ Complexes

Emmanuelle Teuma,[†] Maxime Loy,[†] Carole Le Berre,[†] Michel Etienne,[‡] Jean-Claude Daran,[‡] and Philippe Kalck*,[†]

Laboratoire de Catalyse, Chimie Fine et Polymères, Ecole Nationale Supérieure des Ingénieurs en Arts Chimiques et Technologiques, 118 route de Narbonne, 31077 Toulouse Cedex 4, France, and Laboratoire de Chimie de Coordination du CNRS, UPR 8241, 205 route de Narbonne, 31077 Toulouse Cedex 4, France

Received May 9, 2003

Addition of $H_2C(3,5\text{-}Me_2pz)_2$ (Bpm*) to $[(\eta^4\text{-}1,5\text{-COD})Rh(acetone)_2]BF_4$ affords the complex $[Bpm^*Rh(COD)]BF_4$, which is carbonylated under mild conditions into $[Bpm^*Rh(CO)_2]BF_4$. One of the CO ligands can be easily displaced by PPh_3, $PMePh_2$, or $P(OMe)_3$. The X-ray structures of $[Bpm^*Rh(CO)_2]BF_4$ and $[Bpm^*Rh(CO)(PPh_3)]BF_4$ have been determined and show a rhodium center in a square-planar environment. These complexes have been fully characterized by infrared and ^1H, ^{13}C, and ^{31}P NMR spectroscopy. They are rather active precursors for the hydroformylation of oct-1-ene. They also promote the hydroaminomethylation reaction of terminal alkenes: i.e., the direct production of alkylamines from successive hydroformylation, condensation of the resulting aldehydes with diethylamine, and hydrogenation of the enamines. (2-Methyloctyl)diethylamine and nonyldiethylamine are obtained from oct-1-ene/H_2/CO/$NHEt_2$ building blocks. The reaction rate can be significantly increased on addition of $[RuH_2(PPh_3)_4]$, which acts presumably as a hydride-donating species.

Introduction

Catalytic couplings of amines with olefins or with alkyl and aryl halides to produce more elaborate amines are some of the most important reactions that remain to be solved, not only from a conceptual point of view but also at an economical level, since very often a pharmaceutical activity is relevant to a nitrogen-containing framework.[1] Three main strategies have been explored in the literature. First, the overall olefin insertion into an N−H bond, namely olefin hydroamination, is recognized as a highly challenging process.[1,2] Late-transition-metal complexes have been found to catalyze this reaction, and mechanistic and synthetic issues have been addressed.[3] The catalytic amination of aryl halides is one of the alternatives which is now becoming more efficient.[4] However, another reaction which promotes a different type of coupling, namely hydroaminomethylation of olefins, is worth considering.[5] This tandem reaction couples the hydroformylation of an olefin with amine condensation of the resulting aldehyde, most of the time followed by the hydrogenation of the resulting enamines or imines. Rhodium complexes are successful in promoting these types of reactions. In addition to simple catalytic mixtures, systems based on more sophisticated nitrogen-containing ligands have become popular.[6] For example, cationic bis(imidazolyl)methane rhodium complexes promote an intramolecular (cyclization) version of the hydroamination reaction.[7] In a somewhat related system, we recently described how $[Tp^{Me2,Cl}Rh(CO)_2]$ preferentially activates photochemically a primary C−H bond as opposed to the N−H bond of $NHiPr_2$, yielding a single diastereomer of $[Tp^{Me2,Cl}RhH(CH_2CH(CH_3)NHiPr)]$.[8] Bis(pyrazolyl)methanes can serve as a bridge between bis(imidazolyl)methane and tris(pyrazolyl)borate ligands. On one hand, bis(pyrazolyl)methanes offer two nitrogen atoms for coordination to rhodium, just like bis(imidazolyl)methanes, whereas the Tp′ ligand is usually coordinated in the κ^3-mode in $[Tp'Rh(CO)_2]$. On the other hand, cationic rhodium precursors such as $[(\eta^4\text{-}1,5\text{-COD})Rh(solv)_2]$ are known to catalyze the hydrogenation of alkenes in the presence of PPh_3.

* To whom correspondence should be addressed. E-mail: Philippe.Kalck@ensiacet.fr.
† Ecole Nationale Supérieure des Ingénieurs en Arts Chimiques et Technologiques.
‡ Laboratoire de Chimie de Coordination du CNRS.

(1) *Applied Homogeneous Catalysis with Organometallic Compounds*; Cornils, B., Herrmann, W. A., Eds.; VCH: Weinheim, Germany, 1996.
(2) Recent reviews: (a) Beller, M.; Müller, T. E. *Chem. Rev.* **1998**, *98*, 675−703. (b) Roundhill, D. M. *Chem. Rev.* **1992**, *92*, 1−27.
(3) (a) Fulton, J. R.; Holland, A. W.; Fox, D. J.; Bergman, R. G. *Acc. Chem. Res.* **2002**, *35*, 44−56. (b) Senn, H. M.; Blöchl, P. E.; Togni, A. *J. Am. Chem. Soc.* **2000**, *122*, 4098−4107. (c) Beller, M.; Trautwein, H.; Eichberger, M.; Breindl, C.; Herwig, J.; Müller, T. E.; Thiel, O. R. *Chem. Eur. J.* **1999**, *5*, 1306−1319. (d) Driver, M. S.; Hartwig, J. F. *J. Am. Chem. Soc.* **1997**, *119*, 8232−8245.
(4) (a) Wolfe, J. P.; Wagaw, S.; Buchwald, S. L. *J. Am. Chem. Soc.* **1996**, *118*, 7215−7216. (b) Driver, M. S.; Hartwig, J. F. *J. Am. Chem. Soc.* **1996**, *118*, 7217−7218.
(5) Eilbracht, P.; Bärfacker, L.; Buss, C.; Hollmann, C.; Kitsos-Rzychon, B. E.; Kranemann, C. L.; Rische, T.; Roggenbuck, R.; Schmidt, A. *Chem. Rev.* **1999**, *99*, 3329−3365.
(6) (a) Fache, F.; Schultz, E.; Tommasino, M. L.; Lemaire, M. *Chem. Rev.* **2000**, *100*, 2159−2231. (b) Togni, A.; Venanzi, L. M. *Angew. Chem., Int. Ed. Engl.* **1994**, *31*, 497−526.
(7) Burling, S.; Field, L. D.; Messerle, B. A. *Organometallics* **2000**, *19*, 87−90.
(8) Teuma, E.; Malbosc, F.; Pons, V.; Leberre, C.; Jaud, J.; Etienne, M.; Kalck, P. *Dalton* **2001**, 2225−2227.

10.1021/om030351x CCC: $25.00
Publication on Web 11/06/2003

Table 1. Crystallographic Data for I-BF_4 and III-BF_4

	I-BF_4	**III**-BF_4
mol formula	$C_{13}H_{16}BF_4N_4O_2Rh$	$C_{36}H_{43}BF_4N_4O_3PRh$
fw	450.04	800.43
shape (color)	flat (yellow)	cubic (orange)
cryst size, mm	0.52 × 0.28 × 0.08	0.50 × 0.50 × 0.40
cryst syst	monoclinic	triclinic
space group	$P2_1/n$	$P\bar{1}$
a, Å	7.7361(9)	10.099(1)
b, Å	11.8804(9)	13.346(2)
c, Å	18.5455(19)	14.955(2)
α, deg	90.0	76.36(1)
β, deg	93.67(1)	75.70(1)
γ, deg	90.0	74.83(1)
V, Å^3	1701.0(5)	1853.4(8)
Z	4	2
F(000)	891	824
ρ (calcd), g cm^{-3}	1.757	1.434
μ(Mo Kα) cm^{-1}	10.595	5.64
diffractometer	Stoe IPDS	
radiation	Mo Kα (λ = 0.710 73)	
temp, K	180(2)	
detector dist, mm	70	60
scan mode	ϕ (oscillation)	ϕ (rotation)
ϕ range, deg	0.0 < ϕ < 200.2	0.0 < ϕ < 250.8
ϕ incr, deg	1.4	1.2
exposure time, min	4	2
2θ range, deg	4.4 < 2θ < 52.2	5.9 < 2θ < 56.3
no. of rflns collected	13 449	22 423
no. of unique rflns	3283	8227
merging factor *R*(int)	0.0277	0.0399
no. of rflns used	2695 ($I > 2\sigma(I)$)	6400 ($I > 2\sigma(I)$)
refinement	*F* (CRYSTALS)	F^2 (SHELXL97)
R1, wR2 ($I > 2\sigma(I)$)	0.0250, 0.0136	0.0247, 0.0647
R1, wR2 (all data)		0.0284, 0.0665
$(\Delta/\sigma)_{max}$	0.0006	0.012
$\Delta\rho_{min}/\Delta\rho_{max}$	−0.42/0.42	−0.39/0.36
GOF	1.030	1.033
no. of variable params	226	479

We report herein a new synthetic pathway to [Bpm*Rh(CO)$_2$]BF_4 which avoids the use of the perchlorate counterion[9] and the synthesis of [Bpm*Rh(CO)(PR$_3$)]BF_4 complexes with their structural studies. In addition, we present a first approach to the utilization of such compounds in the hydroformylation and hydroaminomethylation of olefins.

Results and Discussion

Study of [Bpm*Rh(CO)$_2$]BF_4 (I-BF_4). Oro and coworkers[9] have described the preparation of the cation [Bpm*Rh(CO)$_2$]$^+$, isolated as its [RhCl$_2$(CO)$_2$]$^-$ salt, which shows its own ν_{CO} bands at 2075 and 1985 cm^{-1} in the infrared spectrum, via addition of H_2C(3,5-Me$_2$-pz)$_2$ (Bpm*) to [Rh$_2$(μ-Cl)$_2$(CO)$_4$]. The complex [Bpm*Rh(CO)$_2$]ClO_4 (**I**-ClO_4) has also been isolated, and two ν_{CO} stretching frequencies at 2100 and 2035 cm^{-1} in Nujol mull have been reported.[9] We have found that **I**-BF_4 can be prepared by carbonylation of [Bpm*Rh(COD)]BF_4, under ambient conditions, the latter being obtained by addition of $AgBF_4$ to an acetone solution of [Rh$_2$(μ-Cl)$_2$(COD)$_2$]. **I**-BF_4 shows *four* strong ν_{CO} stretching bands at 2092, 2065, 2032 and 1985 cm^{-1} in KBr pellets and *two* bands in dichloromethane solutions (2101 and 2042 cm^{-1}). Similar results are observed in reflectance spectra.

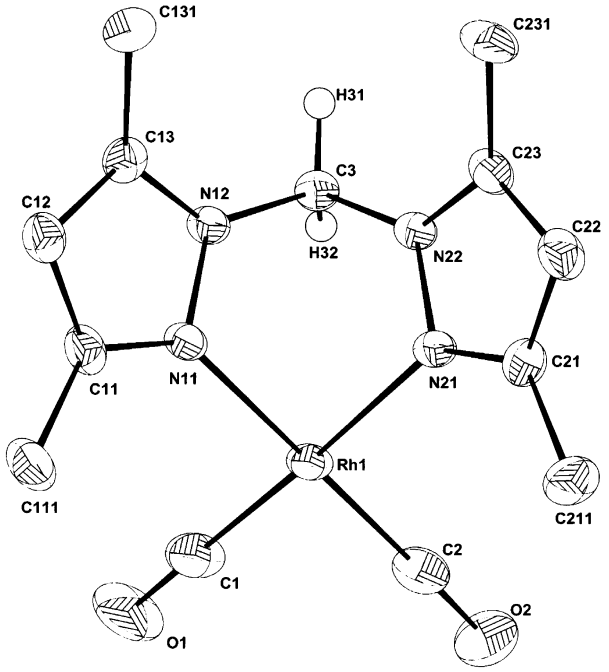

Figure 1. ORTEPIII view of **I**-BF_4 with the atom-labeling scheme. Ellipsoids represent 50% probability. Selected bond lengths (Å) and angles (deg): C(1)−Rh(1), 1.865(2); C(2)−Rh(1), 1.860(3); N(11)−Rh(1), 2.0834(18); N(21)−Rh(1), 2.0888(17); C(1)−O(1), 1.122(3); C(2)−O(2), 1.127(3); N(11)−N(12), 1.365(2); N(21)−N(22), 1.373(2); N(12)−C(3), 1.445-(3); N(22)−C(3), 1.450(3); C(2)−Rh(1)−C(1), 87.82(11); N(21)−Rh(1)−C(2), 93.95(9); N(21)−Rh(1)−N(11), 85.76-(7); N(11)−Rh(1)−C(1), 92.53(9); N(21)−Rh(1)−C(1), 176.79-(9); N(11)−Rh(1)−C(2), 178.6(1).

To clarify these apparent discrepancies, crystals of **I**-BF_4 were grown from an acetone/heptane/diethyl ether solution and analyzed by X-ray diffraction. The X-ray data collection and processing parameters for **I**-BF_4 are given in Table 1. Bond distances and angles of interest are in the classical range and are reported in the caption of Figure 1.

I-BF_4 crystallizes in the space group $P2_1/n$, and the cell contains four asymmetric units consisting of one mononuclear cationic entity and one BF_4 anion. For the discrete cation, the rhodium atom is in a square-planar environment, as shown in Figure 1. The Bpm* entity acts as a chelating ligand, and the four nitrogen atoms and the rhodium and carbon (CH_2) atoms adopt a boat conformation, reminiscent of that observed in the previously described [Bpm*Rh(COD)]ClO_4.[9] The angles between the two CO ligands is 87.82(11)°, in accord with the nearly equal intensities of the two ν_{CO} bands in the solution IR spectra.

The four ν_{CO} bands observed in the solid-state infrared spectra are thus best accounted for by the so-called correlation field approximation, in which the four cations of the unit cell are treated as the vibrating unit, subject to symmetry restrictions arising from the symmetry of the entire unit cell. Due to the presence of the inversion center, only the four antisymmetric C−O stretching vibrations should be observed in the crystal from the eight CO's present in the unit cell.[10] Recall that the importance of this effect is virtually unpredictable.

(9) Oro, L. A.; Esteban, M.; Claramunt, R. M.; Elguero, J.; Foces-Foces, C.; Cano, F. H. *J. Organomet. Chem.* **1984**, *276*, 79−97.

(10) *Chemical Applications of Group Theory*; Cotton, F. A., Ed.; Wiley: New York, 1990; p 342.

Thus, carbonylation of [Bpm*Rh(COD)]BF_4 provides exclusively the mononuclear complex [Bpm*Rh$(CO)_2$]-BF_4, and the four ν_{CO} bands observed in the solid state are not explained by the presence of $[RhCl_2(CO)_2]^-$ but are due to solid-state effects.

CO Substitution Reactions by an Amine or a Phosphine. I-BF_4 does not react cleanly with amines. Monitoring the reaction of **I**-BF_4 with NH*i*Pr_2, morpholine, $NHEt_2$, or piperidine by infrared spectroscopy shows that 1 equiv of amine does not displace any CO ligand at room temperature. In the presence of excess amine, the yellow solution turns rapidly to brown, the CO ligands being evolved. No well-defined species could be isolated from these solutions. NMR data show the presence of free Bpm*, and amine chemical shifts are consistent with their coordination to rhodium. Since no hydride type signals are observed, N−H bond activation remains elusive in these systems. With a large excess of diethylamine, deposition of abundant quantities of black rhodium accompanies CO and Bpm* decoordination.

Trimethylphosphine or dimethylphenylphosphine does not substitute any CO ligand in the complex **I**-BF_4, even under prolonged reaction times, as ascertained by infrared and ^{1}H NMR spectroscopy. In contrast, methyldiphenylphosphine, triphenylphosphine, and trimethyl phosphite as well lead to the monosubstituted complexes [Bpm*Rh(CO)($PMePh_2$)]BF_4 (**II**-BF_4), [Bpm*Rh(CO)-(PPh_3)]BF_4 (**III**-BF_4), and [Bpm*Rh(CO){$P(OMe)_3$}]BF_4 (**IV**-BF_4), respectively. In CH_2Cl_2 solution they present a single ν_{CO} band at 2003, 2008, and 2022 cm^{-1}, respectively, in accord with a mononuclear geometry and in agreement with the decreasing basicity of the phosphorus ligands. These observations suggest that substitution could occur through a pentacoordinated transition state; the Bpm* ligand should occupy both an axial and an equatorial position of a TBP geometry. Considering for instance that the incoming ligand approaches the axial position trans to the other axial pyrazolyl ligand, then as long as its π-back-donation properties accommodate the σ trans-influence of the pyrazolyl group, the substitution can occur. This is the case for less basic ligands such as $P(OMe)_3$, PPh_3, and $PMePh_2$. However, when the ligand is a strong σ-donor such as an amine or PMe_2Ph and PMe_3, coordination does not occur and CO substitution is not observed.

II-BF_4, **III**-BF_4, and **IV**-BF_4 are inert toward the substitution of the second CO ligand. In the [Tp′Rh-(CO)L] case (L = phosphines, phosphites) an excess of phosphorus ligand was not able to displace the second CO, the pyrazolyl groups being progressively removed from the coordination sphere.[11] In the present case, both pyrazolyl groups of Bpm* remain coordinated to the rhodium center.

X-ray Structural Studies of [Bpm*Rh(CO)(PPh_3)]-BF_4·2(acetone) (III-BF_4). The X-ray data collection and processing parameters for **III**-BF_4 are given in Table 1. Relevant bond distances and angles, and a view of the molecule, are shown in Figure 2 and its caption. The rhodium atom is in its usual square-planar arrangement and is bonded to two N atoms of the H_2C(3,5-

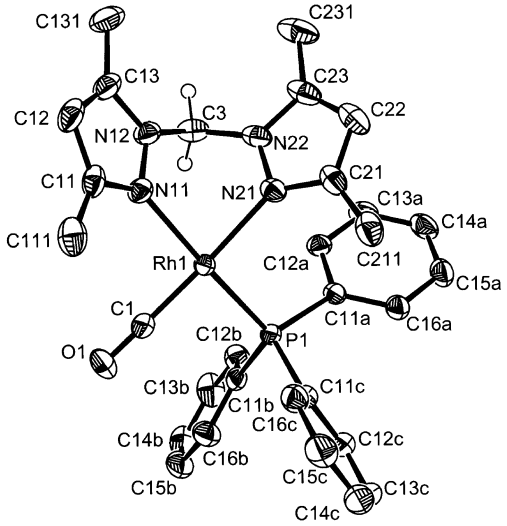

Figure 2. ORTEPIII view of **III**-BF_4 with the atom-labeling scheme. Ellipsoids are drawn at 50% probability. Selected bond lengths (Å) and angles (deg): C(1)−Rh(1), 1.814(2); P(1)−Rh(1), 2.2542(9); N(11)−Rh(1), 2.1110(18); N(21)−Rh(1), 2.1142(17); C(1)−O(1), 1.139(3); C(11a)−P(1), 1.821(2); C(11b)−P(1), 1.836(2); C(11c)−P(1), 1.816(2); N(11)−N(12), 1.365(3); N(21)−N(22), 1.363(3); C(1)−Rh-(1)−N(11), 94.58(8); N(11)−Rh(1)−N(21), 82.62(7); C(1)−Rh(1)−P(1), 87.87(7); N(21)−Rh(1)−P(1), 94.89(5).

$Me_2pz)_2$ ligand, to the C atom of the CO group, and to the phosphorus atom of the PPh_3 ligand.

The Rh distances to the coordinated N atoms (2.1110-(18) and 2.1142(17) Å) are close to those in the literature (2.111(8) and 2.097(7) Å) for [BpmRh(COD)]ClO_4.[9] The Rh(1)−C(1) and Rh(1)−P(1) (1.814(2) and 2.2542(9) Å) distances are comparable to those found for the square-planar derivative [Tp*Rh(CO)(PPh_3)] (Rh−C = 1.824-(6) Å, Rh−P = 2.272(2) Å). The two Rh−N distances of the pyrazolyl groups bonded to the metal center of 2.108-(4) and 2.119(5) Å compare well with those determined here.[12] Similarly, [Tp*Rh(CO)(PR_3)] complexes in which the phosphine ligands are PMe_3 and $PMePh_2$ present bond distances near those of **III**-BF_4.[13] There is almost no distortion around the rhodium atom from the square plane, N(11) being 0.21 Å away from the mean plane calculated from the five atoms C(1), P(1), N(21), N(11), and Rh(1). The six-membered cycle containing the Rh-(1), N(11), N(12), C(3), N(22), and N(21) atoms adopts a boat conformation, with the rhodium atom and the CH_2 group being in the upper positions.

NMR Studies of Complexes I-BF_4−IV-BF_4. ^{1}H NMR spectra of acetone solutions of the dicarbonyl complex **I**-BF_4 show two methyl signals which are consistent with a C_s symmetry, each signal being integrated for six protons at δ 2.47 and 2.59. {^{1}H,^{1}H} and {^{1}H,^{13}C} 2D spectra show no coupling between the methyls at the 5-position and the CH_2 group, so that the signals cannot be definitely ascribed. The CH_2 group shows a broad, poorly resolved signal centered at δ 6.70, indicating an AB system in dynamic exchange. The two CH's of the pyrazoles present a singlet at δ 6.31. ^{13}C NMR spectrum is in agreement with the C_s symmetry

(11) Paneque, M.; Sirol, S.; Trujillo, M.; Carmona, E.; Gutiérrez-Puebla, E.; Monge, M. A.; Ruiz, C.; Malbosc, F.; Leberre, C.; Kalck, P.; Etienne, M.; Daran, J. C. *Chem. Eur. J.* **2001**, *7*, 3868−3879.

(12) Connelly, N. G.; Emslie, D. J. H.; Metz, B.; Orpen, A. G.; Quayle, M. J. *J. Chem. Soc., Chem. Commun.* **1996**, 2289−2290.

(13) Malbosc, F.; Chauby, V.; Leberre, C.; Etienne, M.; Daran, J. C.; Kalck, P. *Eur. J. Inorg. Chem.* **2001**, 2689−2697.

Table 2. Catalyzed Hydroformylation of Oct-1-ene[a]

	oct-1-ene conversn, %	internal octene, %	yield in aldehyde, % (L:B)	time
[Bpm*Rh(CO)(PPh_3)]BF_4 (**III**-BF_4)	98	5	95 (83:17)	3 h
[Bpm*Rh(CO)(PPh_3)]BF_4 + [$RuH_2(PPh_3)_4$] (**III**-BF_4 + [Ru])	95	5	95 (75:25)	40 min
[Bpm*Rh$(CO)_2$]BF_4 (**I**-BF_4)	74	75	25 (60:40)	3 h
[Bpm*Rh(CO)($PMePh_2$)]BF_4 (**II**-BF_4)	92	20	80 (65:35)	3 h
[Bpm*Rh(CO){$P(OMe)_3$}]BF_4 (**IV**-BF_4)	7	82	18 (65:35)	3 h

[a] Experimental conditions: 0.25 mmol of [Rh]BF_4, excess of $PMePh_2$ for **II**-BF_4, PPh_3 for **III**-BF_4, and $P(OMe)_3$ for **IV**-BF_4 (P:Rh = 5), 40 mmol of oct-1-ene, 40 mL of THF, 80 °C, 5 bar.

for **I**-BF_4 and the two CO ligands give a doublet at δ 183.1 ($^1J_{Rh-C}$ = 69 Hz).

The ^{1}H NMR spectrum of **III**-BF_4, recorded at 400 MHz, clearly shows the presence of three methyls in almost the same magnetic environment at δ 2.46, 2.53, and 2.56. The fourth methyl group at δ 1.54 is presumably shielded by one phenyl group of the PPh_3 ligand. Following the numbering scheme of Figure 2, this shielded signal could be ascribed to C(211). The CH_2 group leads to an AB system at δ 6.94 with $^2J_{H-H}$ = 15 Hz. A ^{31}P{^{1}H} NMR doublet has been detected at δ 44.4 ($^1J_{Rh-P}$ = 159 Hz). The rhodium shift is at δ −91.4 with the same Rh−P coupling constant. The CO ligand shows a ^{13}C NMR doublet at δ 188.6 ($^1J_{Rh-C}$ = 71 Hz).

Complexes **II**-BF_4 and **IV**-BF_4, which contain $PMePh_2$ and $P(OMe)_3$, respectively, have also been characterized by ^{1}H, ^{13}C, and ^{31}P NMR. The signals are in agreement with a structure analogous to that of **III**-BF_4. As observed in the X-ray structure, the two hydrogen atoms on C(3) are in different environments. One is strongly influenced by the close vicinity to the rhodium metal (Rh(1)···H = 2.80 Å), which explains the AB system observed in the ^{1}H NMR spectrum. In the ^{13}C NMR spectrum of complex **II**-BF_4, coupling between the ^{13}CO carbon atom and the phosphorus atom gives a doublet of doublets centered at δ 189.0 ($^1J_{Rh-C}$ = 73; $^2J_{P-C}$ = 23 Hz) for the CO ligand. The ^{103}Rh shifts in **II**-BF_4 and **IV**-BF_4 have been measured at δ −175.4 and −258.9, respectively.

Hydroformylation Reaction of Oct-1-ene. Neutral rhodium complexes, particularly [$HRh(CO)(PPh_3)_3$],[14] are frequently involved in catalytic hydroformylation reactions. We have explored this reaction under low-pressure conditions in order to determine the activity and selectivity of complexes **I**-BF_4−**IV**-BF_4 (Table 2).

Under 5 bar of a 1:1 mixture of H_2 and CO and at 80 °C, oct-1-ene is consumed within 3 h in the presence of the system [Bpm*Rh(CO)(PPh_3)]BF_4/4PPh_3. Some isomerization of the starting material occurs, since the resulting mixture contains 5% of internal octenes, in addition to 95% of aldehydes, with a 83:17 ratio of linear to branched (L:B) isomers (GC). We did not observe any hydrogenation of the alkene or of the aldehydes.

Under identical experimental conditions, and with no additional phosphorus ligand, the dicarbonyl complex **I**-BF_4 is somewhat less active (74% conversion of oct-1-ene, internal octenes (75%), nonanals (25%)). Longer reaction times or higher pressures have little influence on the course of the reaction. Similarly the activity of **IV**-BF_4, in the presence of 4 equiv of $P(OMe)_3$, has been considered. This system presents a poor catalytic activity (7% conversion of oct-1-ene, 82% internal octenes, 18% aldehydes (65:35)). [Bpm*Rh(CO)($PMePh_2$)]BF_4 (**II**-BF_4) + 4$PMePh_2$ displays a catalytic activity slightly lower than that of **III**-BF_4 and provides a 92% conversion of oct-1-ene, 20% of internal octene, and 80% of aldehydes with a L:B ratio of 65:35.

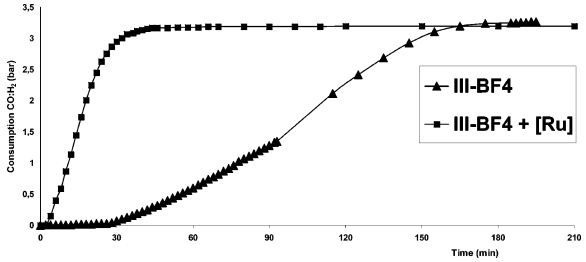

Figure 3. Consumption of CO/H_2 over time.

Thus, for these cationic complexes, the optimum activity as a function of the ligand basicity is rather sharp. The best results are obtained with the classical PPh_3 ligand. High yields of isomerized product indicate that CO migratory insertion is not fast enough as compared to the β-elimination reaction, which restores an alkene from the alkylrhodium species.

Plots of conversion versus time for the complex **III**-BF_4 (Figure 3) present a relatively long induction period of ca. 30 min. Presumably, the likely formation of a dihydride species is a slow process. Another explanation could have been the formation of [$HRh(CO)(PPh_3)_3$], which would have then been responsible for the catalytic activity. However, we have never detected any trace of this hydrido species after reaction. It is worth mentioning that the reaction requires an excess of PPh_3 to prevent the formation of the dicarbonyl complex [Bpm*Rh$(CO)_2$]BF_4, which would have shown its own catalytic activity, and particularly an extended isomerization process. In addition, in the case of **IV**-BF_4, the classical hydrido complex should not be formed, since the complexes [$HRh(CO)\{P(OR)_3\}_3$] are known to be very active at low pressure and to provide an L:B ratio of greater than 6.[15]

[$RuH_2(PPh_3)_4$], which is known to be a good hydrogenation catalyst, has been used as a potential hydride donor (Rh:Ru = 2) in the present hydroformylation reaction. Under otherwise identical experimental conditions, the ruthenium complex alone was seen to be inactive. As shown in Figure 3, the kinetic curve presents a significantly shorter induction period (ca. 4 min) and 95% of oct-1-ene is converted within 40 min.

(14) Jardine, F. H. *Polyhedron* **1982**, *1*, 569 and references therein.

(15) (a) Pruett, R. L.; Smith, J. A. *J. Org. Chem.* **1969**, *34*, 327−330. (b) van Leeuwen, P. W. N. M.; Roobeck, C. F. *J. Organomet. Chem.* **1983**, *258*, 343−350. (c) For an overview on hydroformylation catalyzed by rhodium phosphite complexes see: *Rhodium Catalyzed Hydroformylation*; van Leeuwen, P. W. N. M., Claver, C., Eds.; Kluwer Academic: Dordrecht, The Netherlands, 2000; Chapter 3.

Table 3. Catalyzed Hydroaminomethylation of Oct-1-ene by Diethylamine[a]

	oct-1-ene conversn, %	yield in aldehydes (L:B)	yield in enamine, % (L:B)	yield in amine, % (L:B)	yield in internal octene, %
[Bpm*Rh(CO)(PPh_3)]BF_4 (**III**-BF_4)	95	35 (52:48)	24 (90:10)	37 (72:28)	4
[Bpm*Rh$(CO)_2$]BF_4 (**I**-BF_4)	67			85 (62:38)	15
[Bpm*Rh$(CO)_2$]BF_4 + [$RuH_2(PPh_3)_4$] (**I**-BF_4 + [Ru])	99	35 (39:61)	33 (94:6)	30 (72:28)	2

[a] Experimental conditions: 0.13 mmol of [Rh]BF_4, excess of PPh_3 (P:Rh = 5) for **I**-BF_4, 37.7 mmol of oct-1-ene, 56.55 mmol of $NHEt_2$, 35 mL of THF, 80 °C, 12 bar, time 6 h.

Scheme 1. Successive Steps of the Hydroaminomethylation Reaction

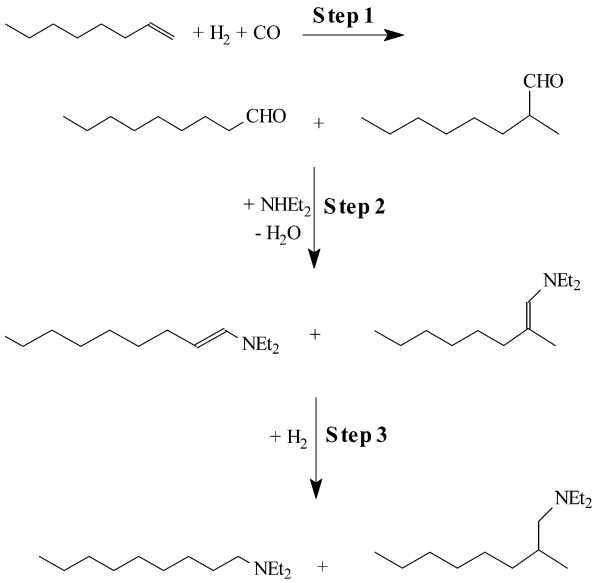

The main role of the ruthenium complex is presumably to activate H_2, providing a $RuH_2(PPh_3)_x$ species (or a $RuH_2(CO)_y(PPh_3)_z$ species under a CO atmosphere), followed by a hydride transfer to rhodium. It is interesting to compare the first two experiments of Table 2, since the isomerization of oct-1-ene is the same (5%) and the reaction was analyzed at roughly the same conversion (98 vs 95%). Similarly, the yields in aldehydes were in both cases 95%. The main difference stems from the regioselectivity. With rhodium alone it is 83:17, whereas for the [Rh−Ru] system it decreases to 75:25. Thus, the role of cocatalyst of the ruthenium complex is essentially revealed in the activation of dihydrogen and presumably for the formation of the alkyl species through a hydride transfer to rhodium. Turnover frequencies are significantly higher with the mixed [Rh−Ru] system, for instance 228 h^{-1} at 40 min as compared to 52 h^{-1} at 180 min for **III**-BF_4 alone, at the same conversion. We can reasonably suppose that rhodium alone drives the last catalytic steps.

Hydroaminomethylation Reaction of Oct-1-ene with Diethylamine. We have examined the activity of **III**-BF_4 in the cascade reaction of hydroformylation, condensation of the resulting aldehydes with diethylamine, and hydrogenation of the enamines into the saturated amines, usually called hydroaminomethylation (Scheme 1).

This reaction, discovered by Reppe in 1949, usually requires high pressures.[5,16] Two recent papers summarize the activity of ruthenium complexes, i.e., [$RuCl_2(C_6H_6)]_2$,[17] or ruthenium−rhodium mixed species generated in situ.[18] These systems work at high temperatures and pressures (120−150 °C, 55−150 bar of CO: $2H_2$, respectively). We have previously obtained significant rates in the same reaction at 18 bar and 80 °C starting from a dinuclear rhodium precursor.[19]

The results of our present studies are summarized in Table 3.

Under 12 bar of an equimolar mixture of CO and H_2 at 80 °C and for 6 h in THF, the complex **III**-BF_4 (substrate to catalyst molar ratio 290) converts 95% of the oct-1-ene. Longer reaction times give the same general trends: 4% of internal octenes, 35% of aldehydes (52:48), 24% of enamines (90:10), and 37% of the saturated amines (72:28) are formed. As expected, if condensation of $NHEt_2$ occurs faster with nonanal than with 2-methyloctanal, the L to B ratio for the amines is rather high. Thus, the hydrogenation of the enamines, step 3 of Scheme 1, is slow, but curiously such a kinetics would give low amounts of the aldehyde, since the condensation (step 2) is generally considered as easy.[20]

To improve the hydrogenation step of the enamines, we have tested the reactivity of the dicarbonyl complex **I**-BF_4, even if its performances in the hydroformylation reaction were lower than those of **III**-BF_4. Pleasingly, the catalytic reaction with **I**-BF_4 in THF results in the exclusive formation of the saturated amines. The rate of oct-1-ene conversion is indeed lower than with **III**-BF_4, but as shown in Table 3, the yield in amines is much higher (85%), even though we observed 15% of isomerized octene. We conclude that precursor **I**-BF_4 accelerates the hydrogenation of the two enamines as compared to complex **III**-BF_4.

Previous results in this laboratory have shown that the addition of ethanol improves significantly the yields in amines.[19] For **I**-BF_4, this effect has not been observed. The slight increase in the conversion of oct-1-ene is accompanied by isomerization (25% of internal octenes). Ethanol addition on **III**-BF_4 has no effect on the yields or selectivities.

[$RuH_2(PPh_3)_4$] assists the catalytic activity of **I**-BF_4 and influences the selectivity in amines. The effect is somewhat more difficult to analyze, since it introduces a PPh_3 ligand. After 80 min, 99% of oct-1-ene is transformed with little isomerization (1% internal octenes). The mixture of products contains 45% of the aldehydes, 32% of the enamines, and 22% of the expected amines. Increasing the reaction time to 6 h does not significantly modify this breakdown, since 35% of aldehydes are present, 33% of enamines, and 30% of

(16) Reppe, W. *Experientia* **1949**, *5*, 93.

(17) Schaffrath, H.; Keim, W. *J. Mol. Catal. A* **1999**, *140*, 107−113.

(18) Schulte, M. M.; Herwig, J.; Fischer, R. W.; Kohlpaintner, C. W. *J. Mol. Catal. A* **1999**, *150*, 147−153.

(19) Baig, T.; Molinier, J.; Kalck, P. *J. Organomet. Chem.* **1993**, *455*, 219−224.

(20) *Advanced Organic Chemistry*, 3rd ed.; March, J., Ed.; Wiley-Interscience: New York, 1985.

amines. We propose that the β-H elimination reaction, which accounts for the primary formation of oct-2-ene, is slower than the CO migratory insertion. We have no information to explain why this new system hydrogenates the enamines so slowly. We have checked that the reaction medium still contains diethylamine. Thus, we suspect that the bimetallic catalytic system inhibits the aldehyde−amine condensation.

The role of ruthenium, either in hydroformylation or in hydroaminomethylation, appears very interesting, and separate studies are in progress to understand the exact implication of both metals.

General Conclusion

The complex [Bpm*Rh(COD)]BF_4 can be prepared in high yields from [$Rh_2(\mu\text{-Cl})_2(COD)_2$], and its carbonylation under mild conditions provides the complex [Bpm*Rh$(CO)_2$]BF_4, which is a mononuclear dicarbonyl cationic species both in solution and in the solid state. Monocarbonyl complexes [Bpm*Rh(CO)(PR_3)]BF_4 have been synthesized with moderately donating ligands (PR_3 = $PMePh_2$, PPh_3 $P(OMe)_3$) but not with more electron releasing ligands.

These complexes are precursors for the low-pressure hydroformylation of oct-1-ene (particularly [Bpm*Rh(CO)(PPh_3)]BF_4) and, quite interestingly, for the hydroaminomethylation of oct-1-ene in the presence of diethylamine (particularly [Bpm*Rh$(CO)_2$]BF_4). Addition of a hydride-donating complex such as [$RuH_2(PPh_3)_4$] dramatically increases the rate of the hydroformylation. For the hydroaminomethylation reaction, the situation is more contrasted. The overall rate is faster, and the isomerization is almost suppressed, but the system remains very slow for both the formation of enamines and their hydrogenation. Presumably ruthenium transfers a hydride ligand to rhodium. Work is in progress to identify this step and to gain a better knowledge of the mechanism of this reaction.

Experimental Section

General Procedures. All manipulations were performed under a dry, oxygen-free nitrogen or argon atmosphere using standard Schlenk techniques. Dichloromethane was dried and distilled over CaH_2; THF and Et_2O were dried over Na/benzophenone. Diisopropylamine was distilled and dried over KOH. Microanalyses were by the ENSIACET. Infrared spectra were recorded on a Perkin-Elmer Model 1710 instrument. NMR spectra were recorded at 25 °C on a Bruker AMX 400 MHz spectrometer. The ^1H and $^{13}C\{^1H\}$ resonances of the solvent were used as the internal standards, but the chemical shifts are reported with respect to TMS. ^{31}P shifts were referenced to external 85% H_3PO_4; $\Xi(^{103}Rh)$ = 3.16 MHz. Kinetic runs for hydroformylation and hydroaminomethylation reactions were performed at constant pressure and temperature in a thermostated reactor. Solid reactants were placed in a 150 mL stainless steel autoclave, which was evacuated by means of a vacuum pump prior to the introduction of the liquid mixture under nitrogen. The reactor was then pressurized with a CO:H_2 = 1:1 mixture and heated to 80 °C, with vigorous stirring of the reaction solution (800 rpm). The consumption of the gaseous mixture was monitored at regular intervals by a pressure gauge until it stopped. The autoclave was then cooled to room temperature and the pressure released. The resulting homogeneous solution was analyzed by GC and IR spectroscopy. Gas chromatography (GC) analysis was performed on a Carlo Erba HRGC 5160 instrument equipped with a capillary column (DB-5 J and W Scientific, 30 m, i.d. 0.32, film 0.25), with the following temperature program: 50 °C (1 °C/min) then 10 °C/min up to 200 °C.

Typical oct-1-ene hydroformylation conditions were as follows: THF (40 mL), oct-1-ene (4.0×10^{-2} mol, 6.3 mL), catalyst (2.50×10^{-4} mol), 5 bar CO:H_2 = 1:1, 80 °C. In all the kinetic runs with ***II***-BF_4 to ***IV***-BF_4, the amount of added phosphine or phosphite was adjusted so as to operate at a P:Rh molar ratio equal to 5. For the catalytic run performed with the addition of the ruthenium hydride complex, 0.5 equiv of the latter was used.

Typical hydroaminomethylation conditions were as follows: THF (35 mL), oct-1-ene (3.77×10^{-2} mol, 5.9 mL), diethylamine (5.65×10^{-2} mol, 5.9 mL), catalyst (1.33×10^{-4} mol), 12 bar CO:H_2 = 1:1, 80 °C. Bis(3,5-dimethylpyrazolyl)-methane (Bpm*),[21,22] [$Rh_2(\mu\text{-Cl})_2(COD)_2$],[23] and [$RuH_2(PPh_3)_4$] [24] were prepared as described earlier.

Synthesis of [(H_2C(3,5-Me_2pz)$_2$)Rh(COD)]BF_4 Addition of silver tetrafluoroborate (347 mg, 1.78 mmol) in acetone (30 mL) to a suspension of [$Rh_2(\mu\text{-Cl})_2(COD)_2$] (440 mg, 0.89 mmol) in acetone (55 mL) gave an immediate precipitate of silver chloride. The suspension was stirred for 30 min. The precipitate was filtered off, and the filtrate was added to H_2C(3,5-Me_2pz)$_2$ (364 mg, 1.78 mmol) in acetone. The resulting yellow solution was stirred for 20 min and concentrated under reduced pressure to ca. 10 mL. The complex was precipitated as a yellow solid by slow addition of diethyl ether, filtered, and dried under vacuum. Yield: 68% (609 mg, 1.21 mmol). ^1H NMR (400 MHz, acetone-d_6, 25 °C): δ 1.98 (m, 4H, CH_2 of COD), 2.35 (s, 6H, CH_3), 2.51 (s, 6H, CH_3), 2.59 (m, 4H, CH_2 of COD), 4.70 (s, 4H, C*H* of COD), 6.07 (s, 2H, C*H*), 7.29 (AB system, $^2J_{H-H}$ = 15 Hz, 2H, CH_2). $^{13}C\{^1H\}$ NMR (100 MHz, acetone-d_6, 25 °C): δ 10.5 (*C*H_3), 13.7 (*C*H_3), 30.5 (*C*H_2 of COD), 59.4 (*C*H_2), 83.0 (*C*H of COD), 109.0 (*C*H), 143.6 (*C*−CH_3), 152.7 (*C*−CH_3). ^{103}Rh NMR: δ −142.0. Anal. Calcd for $C_{19}H_{28}BF_4N_4Rh$: C, 45.43; H, 5.58; N, 11.16. Found: C, 45.75; H, 5.76; N, 11.20.

Synthesis of [(H_2C(3,5-Me_2pz)$_2$)Rh$(CO)_2$]BF_4 (I-BF_4). Carbon monoxide was bubbled through a solution of [(H_2C(3,5-Me_2pz)$_2$)Rh(COD)]BF_4 (300 mg, 0.60 mmol) in dichloromethane (15 mL) for 30 min, causing a color change from yellow to pale yellow. After concentration under vacuum to ca. 1 mL, diethyl ether was added and a pale yellow solid separated. This solid was filtered off, washed with diethyl ether, and dried under vacuum. Crystallization of the residue from acetone/heptane/diethyl ether at −20 °C gave yellow crystals. Yield: 60% (161 mg, 0.36 mmol). IR (KBr; ν, cm^{-1}): 2092, 2065, 2032, 1985. ^1H NMR (400 MHz, acetone-d_6, 25 °C): δ 2.47 (s, 6H, CH_3), 2.59 (s, 6H, CH_3), 6.31 (s, 2H, C*H*), 6.7 (m, 2H, CH_2). $^{13}C\{^1H\}$ NMR (100 MHz, acetone-d_6, 25 °C): δ 10.6 (*C*H_3), 14.4 (*C*H_3), 58.4 (*C*H_2), 108.7 (*C*H), 145.4 (*C*−CH_3), 154.1 (*C*−CH_3), 183.1 (d, $^1J_{Rh-C}$ = 69 Hz, *C*O). ^{103}Rh NMR: δ −108.8. Anal. Calcd for $C_{13}H_{16}BF_4N_4O_2Rh$: C, 34.70; H, 3.58; N, 12.45. Found: C, 35.09; H, 3.61; N, 12.16.

Synthesis of [(H_2C(3,5-Me_2pz)$_2$)Rh(CO)(PPh_3)]BF_4 (III-BF_4). To a solution of [(H_2C(3,5-Me_2pz)$_2$)Rh$(CO)_2$]BF_4 (100 mg, 0.22 mmol) in dichloromethane was added triphenylphosphine (58.3 mg, 0.22 mmol). The mixture was stirred for 30 min. The yellow solution was concentrated under vacuum to ca. 10 mL, and addition of diethyl ether gave a yellow solid. This solid was filtered off, washed with diethyl ether, and dried in vacuo. Crystallization of the residue from acetone/heptane/diethyl ether at −20 °C gave light orange crystals. Yield: 89% (135 mg, 0.20 mmol). IR (KBr; ν, cm^{-1}): 1998, 1966. ^1H NMR (400 MHz, acetone-d_6, 25 °C): δ 1.54 (s, 3H, CH_3), 2.46 (s, 3H, CH_3),

(21) Trofimenko, S. *J. Am. Chem. Soc.* **1970**, *92*, 5118−5126.
(22) Julia, S.; Sala, P.; Del Mazo, J. M.; Sancho, M.; Ochoa, C.; Elguero, J.; Fayet, J.-P.; Vertut, M.-C. *J. Heterocycl. Chem.* **1982**, *19*, 1141−1145.
(23) Giordano, G.; Crabtree, R. H. *Inorg. Synth.* **1990**, *28*, 88−90.
(24) Linn, D. E. *J. Chem. Educ.* **1999**, *76*, 70−73.

2.53 (s, 3H, CH_3), 2.56 (s, 3H, CH_3), 5.85 (s, 1H, C*H*), 6.25 (s, 1H, C*H*), 6.94 (AB system, $^2J_{H-H}$ = 15 Hz, 2H, CH_2), 7.59 (m, 15H, P*Ph*$_3$). ^{13}C{^{1}H} NMR (100 MHz, acetone-d_6, 25 °C): δ 10.6 (*C*H$_3$), 13.9 (*C*H$_3$), 14.3 (*C*H$_3$), 59.0 (*C*H$_2$), 107.9 (*C*H), 108.7 (*C*H), 131.9 (m, P*Ph*$_3$), 144.8 (*C*−CH$_3$), 153.5 (*C*−CH$_3$), 188.6 (d, $^1J_{Rh-C}$ = 71 Hz, *C*O). ^{31}P NMR (160 MHz, acetone-d_6, 25 °C): δ 44.4 (d, $^1J_{Rh-P}$ = 159 Hz, *P*Ph$_3$). ^{103}Rh NMR: δ −91.4 (d, $^1J_{Rh-P}$ = 159 Hz). Anal. Calcd for $C_{30}H_{31}BF_4N_4OPRh$: C, 51.55; H, 3.91; N, 7.63. Found: C, 52.66; H, 4.57; N, 8.19. Despite several recrystallizations from acetone/heptane/diethyl ether, more satisfactory elemental analyses were not obtained.

Synthesis of [(H$_2$C(3,5-Me$_2$pz)$_2$)Rh(CO)(PMePh$_2$)]BF$_4$ (II-BF$_4$). To a solution of [(H$_2$C(3,5-Me$_2$pz)$_2$)Rh(CO)$_2$]BF$_4$ (100 mg, 0.22 mmol) in dichloromethane was added methyldiphenylphosphine (44.45 mg, 0.22 mmol). The mixture was stirred for 30 min. The yellow solution was concentrated under vacuum to ca. 10 mL, and addition of diethyl ether gave a yellow solid. This solid was filtered off, washed with diethyl ether, and dried in vacuo. Yield: 86% (118 mg, 0.19 mmol). IR (KBr; ν, cm^{-1}): 1992, 1977. ^{1}H NMR (400 MHz, acetone-d_6, 25 °C): δ 1.85 (s, 3H, CH_3 of Bpm*), 2.21 (d, $^2J_{P-H}$ = 10 Hz, 3H, P*Me*Ph$_2$), 2.42 (s, 3H, CH_3 of Bpm*), 2.54 (s, 3H, CH_3 of Bpm*), 2.56 (s, 3H, CH_3 of Bpm*), 6.05 (s, 1H, C*H* of Bpm*), 6.27 (s, 1H, C*H* of Bpm*), 6.98 (AB system, $^2J_{H-H}$ = 15 Hz, 2H, CH_2), 7.79 (m, 10H, P*Ph*$_2$). ^{13}C{^{1}H} NMR (100 MHz, acetone-d_6, 25 °C): δ 10.7 (*C*H$_3$), 10.8 (*C*H$_3$), 14.0 (*C*H$_3$), 14.4 (*C*H$_3$), 14.7 (d, $^1J_{P-C}$ = 7 Hz, P*Me*Ph$_2$), 58.6 (*C*H$_2$), 107.7 (*C*H), 108.1 (*C*H), 132.7 (m, P*Ph*$_2$), 143.7 (*C*−CH$_3$), 144.4 (*C*−CH$_3$), 152.2 (*C*−CH$_3$), 152.5 (*C*−CH$_3$), 189.0 (dd, $^1J_{Rh-C}$ = 73 Hz, $^2J_{P-C}$ = 23 Hz, *C*O). ^{31}P NMR (160 MHz, acetone-d_6, 25 °C): δ 30.5 (d, $^1J_{Rh-P}$ = 153 Hz, *P*MePh$_2$). ^{103}Rh NMR: δ −175.4 (d, $^1J_{Rh-P}$ = 153 Hz).

Synthesis of [(H$_2$C(3,5-Me$_2$pz)$_2$)Rh(CO){P(OMe)$_3$}]BF$_4$ (IV-BF$_4$). To a solution of [(H$_2$C(3,5-Me$_2$pz)$_2$)Rh(CO)$_2$]BF$_4$ (100 mg, 0.22 mmol) in dichloromethane was added trimethyl phosphite (27.54 mg, 0.22 mmol). The mixture was stirred for 30 min. This yellow solution was concentrated under vacuum to ca. 10 mL, and addition of diethyl ether gave a yellow solid. This solid was filtered off, washed with diethyl ether, and dried in vacuo. Yield: 77% (92.83 mg, 0.17 mmol). IR (KBr; ν, cm^{-1}): 2019, 1987. ^{1}H NMR (400 MHz, acetone-d_6, 25 °C): δ 2.35 (s, 3H, CH_3 of Bpm*), 2.44 (s, 3H, CH_3 of Bpm*), 2.56 (s, 6H, CH_3 of Bpm*), 3.84 (d, $^3J_{H-P}$ = 13 Hz, 9H, CH_3 of P(OMe)$_3$), 6.21 (s, 1H, C*H* of Bpm*), 6.24 (s, 1H, C*H* of Bpm*), 6.82 (AB system, $^2J_{H-H}$ = 15 Hz, 2H, CH_2 of Bpm*). ^{13}C{^{1}H} NMR (100 MHz, acetone-d_6, 25 °C): δ 10.5 (*C*H$_3$ of Bpm*), 14.2 (*C*H$_3$ of Bpm*), 52.5 (d, $^2J_{P-C}$ = 2 Hz, *C*H$_3$ of P(OMe)$_3$), 58.6 (*C*H$_2$ of Bpm*), 108.1 (*C*H of Bpm*), 108.7 (*C*H of Bpm*), 143.9 (*C*−CH$_3$ of Bpm*), 144.4 (*C*−CH$_3$ of Bpm*), 249.8 (d, $^1J_{Rh-C}$ = 60 Hz, *C*O). ^{31}P NMR (160 MHz, acetone-d_6, 25 °C): δ 135.3 (d, $^1J_{Rh-P}$ = 245 Hz, *P*(OMe)$_3$). ^{103}Rh NMR: δ −258.9 (d, $^1J_{Rh-P}$ = 245 Hz). Anal. Calcd for $C_{15}H_{25}BF_4N_4O_4PRh$: C, 32.99; H, 4.61; N, 10.26. Found: C, 32.51; H, 4.37; N, 9.11.

X-ray Structure Determination. Data for **I**-BF$_4$ and **III**-BF$_4$ were collected on a Stoe IPDS diffractometer equipped with an Oxford Cryostream nitrogen low-temperature device. The final unit cell parameters were obtained by the least-squares refinement of 8000 reflections. Only statistical fluctuations were observed in the intensity monitors over the course of the data collections.

The structures were solved by direct methods (SIR97)[25] and refined by least-squares procedures on F using CRYSTAL[26] for **I**-BF$_4$ and on F^2 using SHELXL-97[27] for **III**-BF$_4$. All H atoms attached to C were introduced in calculations in idealized positions (d(CH) = 0.96 Å) and treated as riding models. The weighting scheme used in the last refinement cycles was $w = w'[1 - \{\Delta F/6\sigma(F_o)\}^2]^2$, where $w' = 1/\sum_1^n A_r T_r(x)$ with three coefficients A_r for the Chebyshev polynomial $A_r T_r(x)$ and x was F_c/F_c(max),[28] for **I**-BF$_4$, whereas the weighting scheme $w = 1/[\sigma^2(F_o^2) + (aP)^2 + bP]$, where $P = (F_o^2 + 2F_c^2)/3$, was used for **III**-BF$_4$. The drawings of the molecules (Figures 1 and 2) were realized with the help of ORTEP32.[29] Further details of data collection and refinement are listed in Table 1.

Acknowledgment. The Ministère de la Recherche et de la Technologie is gratefully acknowledged for a research grant to E.T. We are indebted to Engelhardt-CLAL for a generous loan of rhodium trichloride.

Supporting Information Available: Tables giving crystallographic data (excluding structure factors) for the structures reported in this paper. This material is available free of charge via the Internet at http://pubs.acs.org. These data have also been deposited with the Cambridge Crystallographic Data Center as Supplementary Publication Nos. CCDC-193814 (**I**-BF$_4$) and CCDC-193815 (**III**-BF$_4$).

OM030351X

(25) Altomare, A.; Burla, M. C.; Camalli, M.; Cascarano, G. L.; Giacovazzo, C.; Guagliardi, A.; Moliterni, A. G. G.; Polodori, G.; Spagn, R. SIR97: A Program for Automatic Solution of Crystal Structures by Direct Methods. *J. Appl. Crystallogr.* **1999**, *32*, 115.

(26) Watkin, D. J.; Prout, C. K.; Carruthers, J. R.; Betteridge, P. W. CRYSTALS Issue 11; Chemical Crystallography Laboratory, University of Oxford, Oxford, U.K., 2000.

(27) Sheldrick, G. M. SHELXL97: Program for Crystal Structure Refinement; University of Göttingen, Göttingen, Germany, 1997.

(28) Prince, E. *Mathematical Techniques in Crystallography*; Springer-Verlag: Berlin, 1982.

(29) Farrugia, L. J. ORTEP-32 for Windows. *J. Appl. Crystallogr.* **1997**, *30*, 565.